A molecular-dynamics study of the dynamic properties of liquid rubidium. I. Collective correlation functions

1994 J. Phys.: Condens. Matter 6 10897

(http://iopscience.iop.org/0953-8984/6/50/004)

J. Phys.: Condens. Matter 6 (1994) 10897–10921. Printed in the UK

A molecular-dynamics study of the dynamic properties of liquid rubidium: I. Collective correlation functions

G Kahl and S Kambayashi†

Institut für Theoretische Physik, Technische Universität Wien, Wiedner Hauptstraße 8-10, A-1040 Wien, Austria

Received 18 February 1994, in final form 30 June 1994

Abstract. We present results of a molecular-dynamics study where we calculated the dynamic structure of six states of liquid rubidium. The systems are chosen along the liquid–gas coexistence curve; four of these states have been considered in a recent neutron-scattering experiment by Winter *et al*. The interatomic forces are based on an Ashcroft empty-core pseudopotential. This present paper—the first of two contributions—contains results for the collective correlation functions. For the dynamic structure factor $S(q,\omega)$ we find for temperatures up to ~1700 K very good quantitative agreement with the experimental results. Discrepancies which we encountered in the high-temperature state (1873 K) may undoubtedly be attributed to the inadequacy of the underlying interaction: near the critical point a metal/non-metal transition occurs for Rb and the interatomic forces (based on mean electronic density) we used are no longer able to describe the complex changes in the electronic structure correctly. We find that the behaviour of the intermediate scattering function near q_p (the position of the main peak in the structure factor $S(q)$) may be very well understood in terms of a simple memory-function model, involving static properties only. The interpretation of both the longitudinal and transverse current correlation functions using reliable hydrodynamic and memory-function models has revealed that, for intermediate- and high-temperature states, the temperature influence enters only via the static moments of the correlation functions while the parameters of the models (which are determined in a least-squares fit to the correlation functions) turn out to be practically temperature independent. Once more we experience that it is extremely difficult to determine elastic and thermodynamic quantities from the computer data of the correlation functions in a reliable and accurate way: the quality of the results may be very sensitive to the underlying model; results obtained via different routes and interpretations may differ substantially and discrepancies with experiment of 10–20% have to be considered as normal.

1. Introduction

In particular during recent years, considerable progress has been made in both experimental and theoretical investigations on the dynamic structure of liquid metals. If we consider only the alkali metals, nearly all elements of this group have been studied in *neutron-scattering* experiments: Li [1, 2], Na [3, 4, 5], Rb [6, 7, 8, 9] and Cs [10, 11, 12]. On the theoretical side, the dynamic properties of liquid alkali metals have been studied by means of *computer* experiments (molecular-dynamics—MD—simulations); such theoretical experiments have been performed mainly on Rb and were started with the pioneering work of Rahman [13, 14] and were followed by studies by Mountain and co-workers [15, 16] and Balucani *et al* [17, 18]: all these investigations considered Rb near the melting point and in the supercooled

† Present address: Computing and Information Systems Centre, Tokai Research Establishment, JAERI, Tokai, Naka, Ibaraki 319-11, Japan.

0953-8984/94/5010897+25$19.50

region; recently, a study on the dynamic properties of liquid Cs just above the melting point has been published by the present authors [19, 20]. Furthermore only recently a systematic study of the dynamic properties of all liquid alkali metals (except for lithium) near the respective melting points [21, 22] and a study on the dynamic properties of liquid lithium [23, 24] have been published. Due to the increased computational power of workstations longer runs and larger ensembles have improved the accuracy of the results substantially. Furthermore, hydrodynamic theories (HF) or a memory-function analysis (MF), or—still more sophisticated—mode-coupling (MC) theories [25, 26] make a better interpretation of the raw computer data (i.e., of the dynamic correlation functions—CFs) possible. We may conclude that both neutron-scattering and computer experiments produce nowadays results of the same degree of accuracy and may be considered as equal partners in studying the dynamic properties of liquids.

The present study has primarily been motivated by the inelastic neutron-scattering experiment on Rb by Winter and co-workers [8, 9]. Their study is of fundamental importance insofar as it represents the *first* investigation on dynamic properties of a liquid metal up to the critical region: the states they have considered are chosen along the coexistence curve and range from intermediate temperatures (1073 K) up to near the critical point. This critical region is in the case of rubidium (and also of caesium) of special interest: almost simultaneously with the liquid/gas transition Rb undergoes a metal/non-metal transition. The critical data of these two elements (e.g., Rb: $T_c = 2017$ K and $\rho_c = 290$ kg m^{-3} [27]) are—in contrast to the lighter alkali metals—found to be within the limits of static temperatures and pressures available in the laboratory. This transition can be inferred from measurements of the electric conductivity, magnetic susceptibility and optical reflectivity [28, 29, 30, 31, 32]. These experimental results indicate the presence of electronic correlation effects which can be considered as the precursors of the metal/non-metal transition. From the experimental results of the *static* structure of expanded liquid Rb and Cs [33, 34] one also finds a nearly constant number of nearest neighbours and an increasing distance of nearest neighbours with rising temperature. In the *dynamic* structure experimentalists observe for low and intermediate temperatures phonon-like collective modes far outside the hydrodynamic region, visible as side peaks or shoulders in $S(q, \omega)$; even beyond q_p (i.e., the position of the main peak in the static structure factor $S(q)$) a shoulder is visible which might be interpreted as an inelastic peak and hence as collective modes 'beyond' q_p (cf. also the experimental study on liquid Cs [10, 11, 12]). However, for the highest temperature investigated (1873 K with a density of about twice the critical density), a change in the shape of $S(q, \omega)$ is observed: a broad side peak develops out of the structureless scattering function observed for lower-temperature states at $q \sim 1$ Å^{-1}. This transition near the critical point must of course be caused by the interaction forces: this is, e.g., reflected in the breakdown of the results obtained in the 'nearly-free-electron' picture for the conductivity of the expanded liquid metals [35, 36], or the failure of simple interatomic forces used when describing the rise of $S(q)$ in the low-q limit [37, 38] via standard liquid-state theories.

The aim of this theoretical study is not only a simple comparison between theoretical and experimental results: the principal aim of this study is rather to find out how the behaviour of dynamic CFs and several elastic and thermodynamic properties change as we expand the system from the melting point up to the critical region seen from the point of view of a computer experiment. A further important motivation for such a study was the fact that several dynamic (both single-particle and collective) CFs may be determined in a computer experiment, but not in a neutron-scattering experiment. Experimental and theoretical results together should then offer a deeper insight into the dynamic behaviour of these Rb states.

In this contribution (which we have split up into two papers for reasons given below),

we have investigated the temperature range from the melting point up to 1873 K, considering six states; four of these states are exactly the same systems as in Winter's experiments. The present study may also be regarded as an extension of earlier investigations on liquid Rb which were primarily concerned with states near the melting point and/or the supercooled regime. The questions we are interested in here are the following: (i) how do the results of the computer experiment compare with the neutron scattering data? (ii) for the case where differences between these two sets of data are encountered, what might be a possible explanation for these discrepancies? and finally, (iii) what can we learn from computer experiments which is not already accessible from real experiment (and vice versa) and hence justifies those rather expensive calculations. We hope to answer these questions satisfactorily in the two papers.

The contribution is split up into two parts: the first paper contains results for the collective CFs, while the second part is devoted to the single-particle CFs. In the first paper we have compiled results of the collective dynamic CFs (i.e., the dynamic structure factor $S(q, \omega)$ and the longitudinal/transverse current CFs $C_{l/t}(q, t)$) and a comparison of the theoretical data with experimental results. The subsequent paper [39] deals entirely with the theoretical results of the single-particle CFs (i.e., the self-dynamic structure factor $S_s(q, \omega)$ and the velocity autocorrelation function—VACF—$\Psi(t)$). However, due to the small incoherent scattering length no experimental results are available for the single-particle CFs.

In this theoretical study the interatomic forces are based on a local pseudopotential (proposed by Ashcroft [40]), using the Ichimaru–Utsumi expression for the exchange–correlation correction [41, 42]. We are well aware of the fact that this potential (along with a classical MD simulation) is not able to describe those complicated changes in the electronic structure which cause the metal/non-metal transition. For the present study we have nevertheless chosen this type of interatomic force: up to now no satisfactory models have been proposed of how to construct interatomic potentials covering the temperature range from the triple point up to the critical region; hence, we rather prefer to use the Ashcroft potential in order to describe *all* states in a coherent manner by the *same* type of interaction. We expect that the failure of this simple model should affect—similarly as in a study on the static structure (Rb: [38])—only the high-temperature state.

The simulation has been performed using a standard microcanonical MD code with the usual periodic boundary conditions; we used throughout 1372-particle ensembles. The equations of motion were integrated over 100 000 time steps Δt (Δt ranging from 3 to 6 femtoseconds).

In this first part of the study we find up to intermediate temperatures very good agreement between the theoretical and experimental results [8, 9]; only for the highest temperature (1873 K) are substantial discrepancies encountered. These differences may be clearly attributed to the underlying interatomic potential, i.e., to a potential which does not account for local variations of the forces arising from critical density fluctuations encountered in the critical region. A similar good agreement with Winter's data [8, 9] and earlier experimental results [6, 7] of the dispersion relation determined from the longitudinal current CFs is observed. The computer data for the dynamic CFs are interpreted in terms of hydrodynamic (HF) and of memory-function (MF-n, n being the number of parameters involved) models. It turns out that the model parameters are—except for the lowest-temperature states—practically temperature independent; temperature effects which are observed for the dynamic CFs must hence enter via the other constituents of these models, i.e., the static moments of the CFs. In conjunction with these observations it is furthermore worthwhile to note that several aspects of the dynamic CFs may often be explained in both a qualitative and quantitative way on the grounds of models based entirely on the static structure. In

contrast to earlier results obtained for dynamic properties of liquid metals near the melting point, we find that for higher temperatures there exists a gap in q-space where neither longitudinal nor transverse collective modes are observed (while for low temperatures these ranges do overlap). Once more we experience that a reliable and accurate determination of thermodynamic and elastic properties from raw computer data turns out to be extremely difficult (i.e., from an extrapolation of generalized q-dependent parameters towards $q = 0$); in a few cases MC approaches have been used to extract such quantities. In general we found that agreement with experimental data is acceptable (i.e., differences between 10 and 20% are encountered); results for the kinetic shear viscosity ν show a remarkably good degree of agreement.

The paper is organized as follows. In the following section we present the interatomic forces of the Rb atoms as well as details about the numerical parameters of the simulation. This section also contains the definitions of the collective dynamic CFs; for a more complete presentation we refer the reader either to our previous study [19, 20] (where we have used exactly the same definitions) or to standard text books [25, 26]. In section 3 we present and discuss our results and compare them with the experimental data, including structure as well as thermodynamic and elastic properties. The paper is concluded with a summary.

2. The model, the simulation and the correlation functions

2.1. *Interatomic forces*

We have studied six different Rb states (denoted henceforward by I–VI), which are characterized by temperatures T and mass densities n; these parameters have been taken from [43] and are compiled in table 1. State I is chosen to be 'near' the system treated by Rahman [13, 14]; states III to VI correspond exactly to the systems which were treated in the experimental study of Winter *et al* [8, 9].

Table 1. Temperature T and mass density n of the six Rb states I to VI investigated in this study. r_{cut} is the cut-off radius for the potential and Δt is the time increment used in the MD simulation (cf. text).

System	T (K)	n (kg m^{-3})	r_{cut} (Å)	Δt (s)
I	350	1460	16.72	5×10^{-15}
II	373	1440	16.76	6×10^{-15}
III	1073	1130	17.44	3×10^{-15}
IV	1373	980	17.80	3×10^{-15}
V	1673	830	18.40	3×10^{-15}
VI	1873	640	19.00	3×10^{-15}

The interatomic forces of the Rb atoms are based on pseudopotential theory: we use the Ashcroft empty-core pseudopotential [40] and the Ichimaru–Utsumi parametrization for the local-field corrections to the dielectric function [41, 42] for reasons discussed in [19, 20]. The core radius of the pseudopotential, r_c, which is the only free parameter of the model, was chosen to be 2.47 au. This choice is justified as follows: (i) this value provides good agreement for the static structure of liquid Rb between theory and experiment [38] over a large temperature range (i.e., up to ~1700 K), (ii) it guarantees a zero-pressure condition for the solid state [44] and (iii) it yields values for the longitudinal and transverse phonon

frequencies of the solid state which are in good agreement both with experimental results [45] and with data obtained via other, more sophisticated pseudopotential methods (such as the generalized pseudopotential theory [46]). The respective values of these frequencies are compiled in table 2. In contrast to state-independent potentials such as the Lennard-Jones systems (LJ) we observe that for higher temperatures the first minimum of the reduced potential again becomes deeper due to the decrease in electron screening of the ion cores; the position of the minimum and hence the position of the main peak in the PDF are found to be rather insensitive to temperature.

Table 2. Longitudinal (L) and transverse (T) phonon frequencies in ps^{-1} for Rb at the Brillouin-zone boundary, calculated from the 'generalized pseudopotential theory' [46] (a) and from this model potential (b) and as obtained from experiment [45] (c).

	(a)	(b)	(c)
L [100]	1.35	1.385	1.464
L [110]	1.49	1.500	1.461
T_1 [100]	0.27	0.340	0.367
T_2 [100]	0.92	0.960	0.977

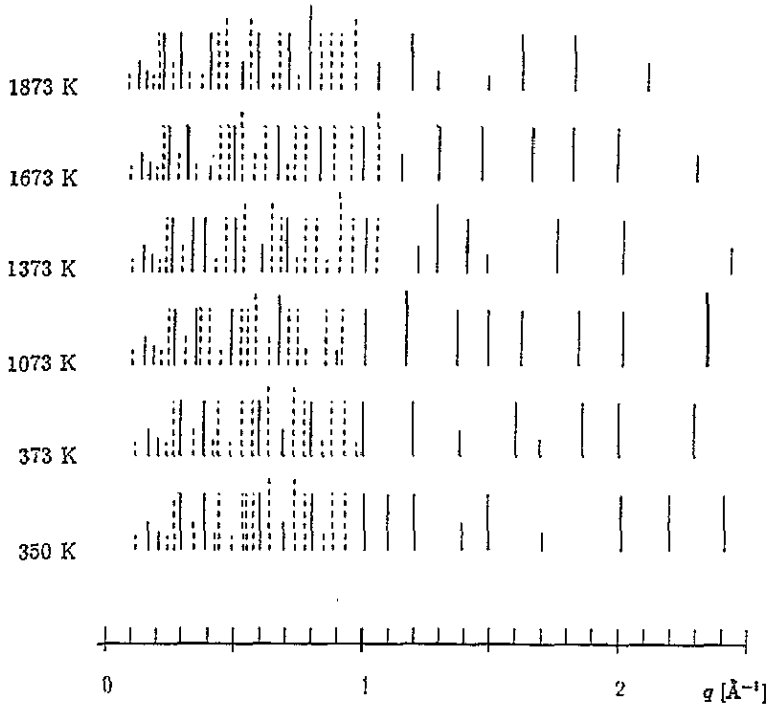

Figure 1. q-vectors considered in the present (full bars) and subsequent paper (full and broken bars) for Rb states I–VI. The height of each bar is proportional to the respective N_q.

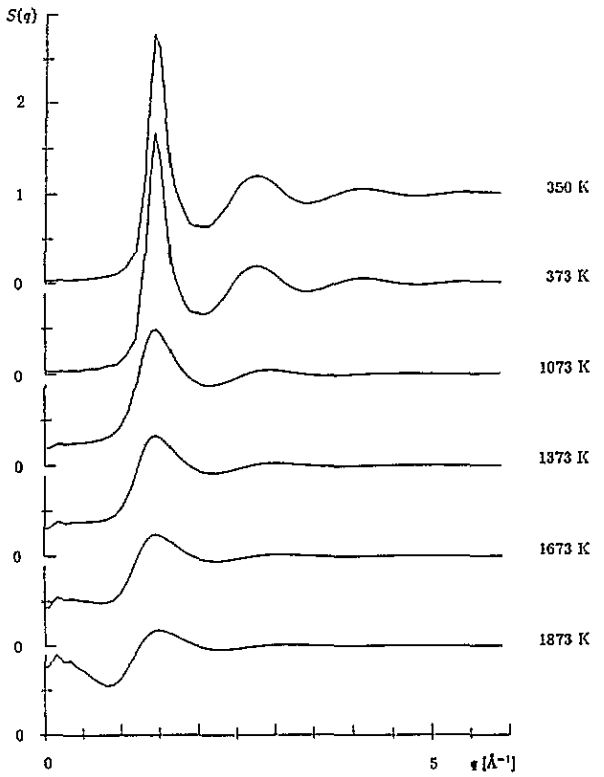

Figure 2. Static structure factors $S(q)$ ($= \omega_0^0(q)$, the zero-order moment of the intermediate scattering function $F(q, t)$) as functions of q for Rb states I–VI.

2.2. *The correlation functions*

Static CFs (i.e., the PDF $g(r)$) were obtained by averaging every 40 Δt. The Fourier transform (FT) of $g(r)$ is the static structure factor $S(q)$. ρ is the number density and M is the mass of the Rb atoms ($n = \rho M$). The position of the main peak of $S(q)$ will be denoted by q_p.

2.3. *The simulation*

The simulation has been performed using a standard microcanonical MD code with the usual periodic boundary conditions; the equations of motion have been integrated by means of a fourth-order predictor–corrector Gear algorithm [47]. For all systems 1372-particle ensembles have been considered. The runs have been performed over 100 000 time steps Δt; Δt varies from 3 to 6 femtoseconds (cf. table 1). Unless an energy conservation for the *entire* MD run of less than 0.01% was achieved the run was discarded. Both static and dynamic CFs were calculated by averaging over time, invoking the ergodic hypothesis of the equality of time and ensemble averaging. Temperature and energy were recorded during the simulation run, which enabled us to obtain further information on the system. The grid size of the tabulated potentials was 0.04 Å. The potentials were truncated at radii r_{cut} which are the respective sixth nodes of $\Phi(r)$ (cf. table 1), representing 32.7 % (I) to 28.3% (VI) of the simulation box length; at these distances the potentials have dropped to 0.3% (I) to 0.17% (VI) of the value of $\Phi(r)$ at the first attractive minimum.

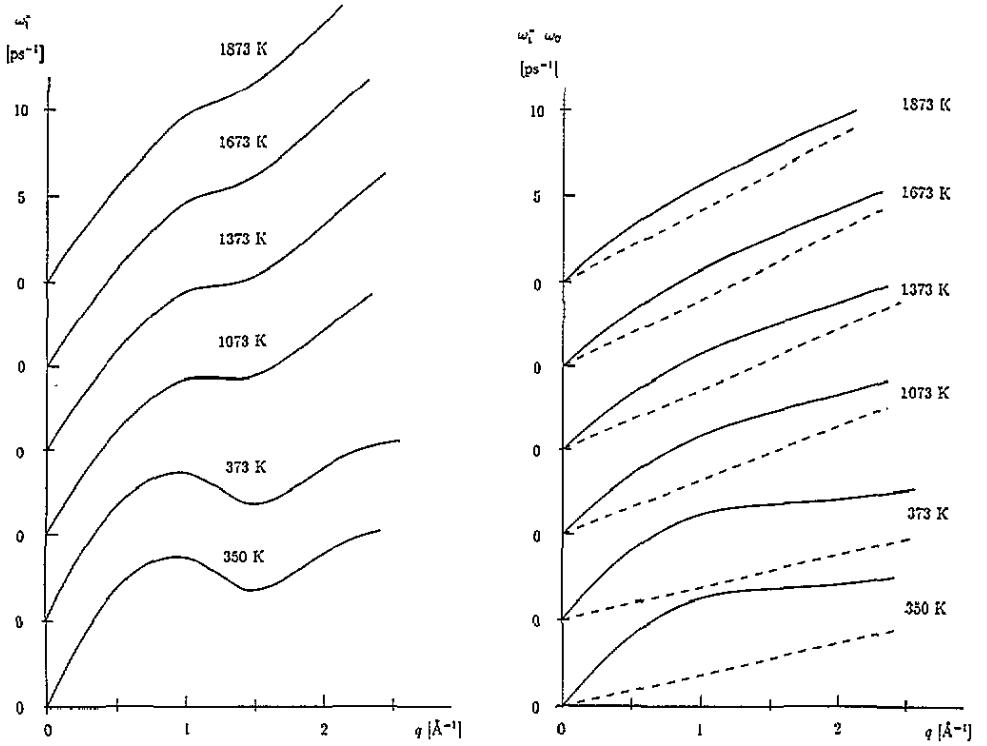

Figure 3. Second-order moments $\omega^*_{l/t}(q) = \sqrt{\omega^2_{l/t}(q)/\omega^2_0(q)}$ (longitudinal—left, transverse—right) as functions of q for Rb states I–VI. The moment $\omega^2_0(q) = (qv_0)^2$ ($v_0^2 = (\beta M)^{-1}$ being the thermal speed) is indicated as a broken line in the right-hand panel.

The dynamic CFs have been calculated as functions of q on a discrete q-grid; these values have to be compatible with the periodic boundary conditions. Due to technical reasons we have not taken into account those q-values with more than 18 directions N_q with the same modulus q. The q-values considered in this study are depicted in figure 1 for systems I to VI; the N_q values range from 4 to 18.

The FT of the density ($\rho_q(t)$) and the current operator ($j_q(t)$) (for details cf. [20, 25]) were recorded every second time step. From these quantities the intermediate scattering function $F(q,t)$ and the longitudinal/transverse current CFs $C_{l/t}(q,t)$ were calculated.These CFs have been recorded over 1024 Δt. The dynamic CFs have been obtained by shifting origins by 4 Δt (cf. equation (7) of [20]). Furthermore an averaging over q-vectors with the same modulus has been performed for the determination of the dynamic CFs. The moments $\omega^n_0(q)$ and $\omega^n_{l/t}(q)$ (of $F(q,t)$ and of the current CFs) were calculated from $\Phi(r)$ and $g(r)$ using the standard relations [20]. Moments involving static CFs of order higher than two (i.e., beyond the PDF) have not been taken into account.

The spectra $C_{l/t}(q,\omega)$ (i.e., the FTs of $C_{l/t}(q,t)$) show for all q-values a maximum for $\omega > 0$, while for $S(q,\omega)$ this maximum may not be resolved for all q-values. These maxima recorded as functions of q are called dispersion relations and will be denoted for the respective CFs by $\omega^m_{l/t}(q)$ and $\omega_B(q)$.

The dynamic CFs have been studied and interpreted in terms of HF and MF models as outlined in [25, 26], using the same notation as in [20]: (i) the HF model for $S(q,\omega)$ (and $C_l(q,\omega)$) contains the following elastic and thermodynamic parameters: $\gamma = C_p/C_v$, the

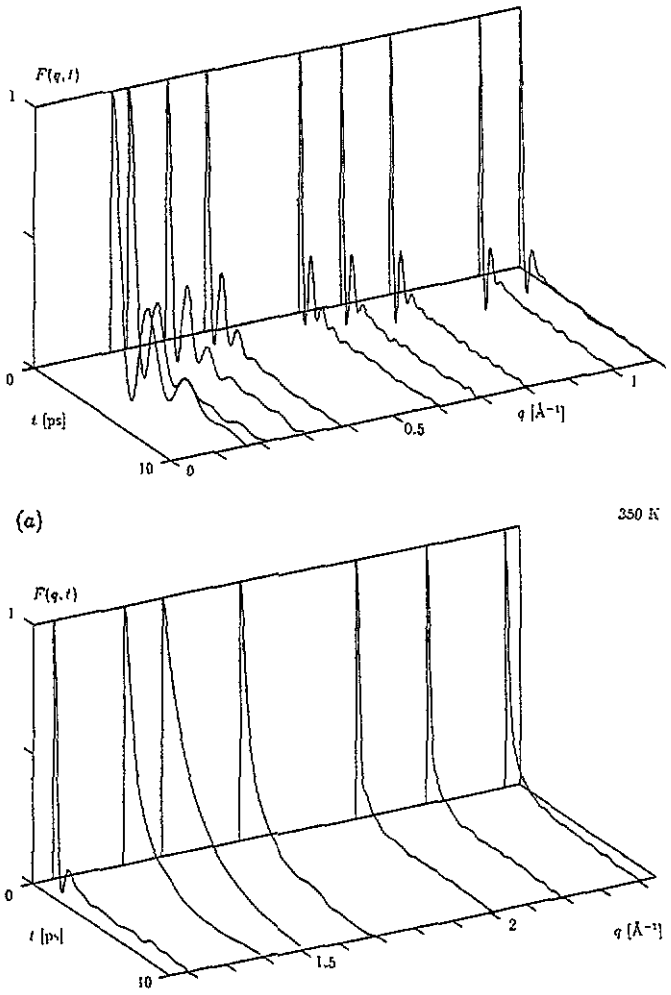

Figure 4. Intermediate scattering functions $F(q,t)$ as functions of q and t for the following Rb states: (a) I (350 K) and (b) IV (1373 K).

ratio of the specific heats, the thermal diffusivity D_T, the sound attenuation coefficient Γ and the adiabatic velocity of sound c_s. The HF model for $C_t(q,\omega)$ contains one single parameter, the kinetic shear viscosity ν ($= \eta/\rho M$, η being the shear viscosity); (ii) for the MF models, one- and three-parameter expressions (MF-1 and MF-3) have been used for both $C_l(q,t)$ and $C_t(q,t)$. In the one-parameter case, the parameters represent relaxation times τ_l (τ_t); the three-parameter models contain one further relaxation time (which turns out to differ from the first one by one or two orders of magnitude) and a mixing parameter α_l (α_t) which weighs the two contributions to the memory. All these parameters are q dependent. From their limit $q \to 0$ (i.e., by extrapolating towards zero), we can extract in the longitudinal case information on D_T, γ and on the longitudinal viscosity η_l; in the transverse case we get results for η (cf. discussion and table VI in [20]).

The specific heat at constant volume C_v and the diffusion constant D have been obtained via standard relations from the temperature fluctuation and the mean square displacement, which were both recorded during the MD runs.

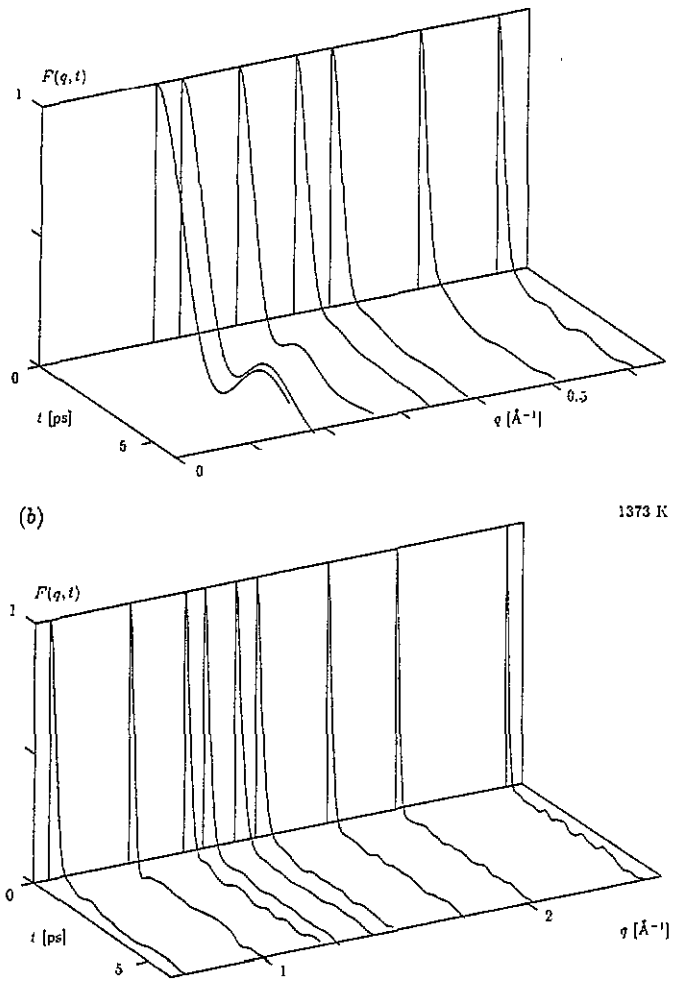

Figure 4. (Continued)

3. Results

3.1. Static correlation functions

In figure 2 we show the static structure factor $S(q)$ for states I–VI. Similarly as in the experimental study [8, 9], we find that the positions of the main maxima in $g(r)$ ($r_p \sim 4.8$ Å) and in $S(q)$ ($q_p \sim 1.45$ Å^{-1}) are practically insensitive to the temperature; Winter has interpreted this by an inhomogeneous expansion of the liquid, since during the expansion the *distance* of nearest neighbours remains unchanged, while the *number* of nearest neighbours decreases substantially. The approach to the critical point is characterized by the onset of a divergence of the experimental $S(0)$; in the theoretical study this divergence is found to be less drastic than in experiment: only a moderate onset of this divergence is visible for the highest temperature. This is mainly due to the inadequacy of the interatomic forces used in the vicinity of the critical point. Such discrepancies between experiment and theory have already been observed in earlier studies on the static structure of expanded liquid Rb and

Cs using different liquid-state methods [38, 48].

The static structure factor $S(q)$ represents also the zero-order moment of the intermediate scattering function $F(q,t)$. The higher-order moments of $F(q,t)$ and of the other collective dynamic CFs are depicted in figure 3: for $\omega_l(q)$ we observe at lower temperatures a pronounced minimum which is smeared out as the temperature is increased, so that we finally observe simply a turning point at 1873 K. The position of the minimum (or the turning point) of $\omega_l^2(q)$ coincides with q_p and hence is rather unaffected by the temperature. A similar behaviour will also be observed for several other functions which we discuss later; these effects are closely related to the so-called de Gennes narrowing [49] observed in $S(q,\omega)$ [50] (or in $F(q,t)$ [51]) near q_p.

3.2. *Dynamic correlation functions*

3.2.1. Intermediate scattering function and dynamic structure factor. In figure 4 we present results for the intermediate scattering function $F(q,t)$ for two chosen temperatures: a drastic change in the behaviour of $F(q,t)$ is observed as we increase the temperature. (i) At 350 K for small q-values pronounced oscillations are found; with increasing q, these oscillations are dampened, and $F(q,t)$ becomes in the vicinity of q_p ($\sim$1.45 Å^{-1}) and for larger q-values a simple, monotonically decreasing function: $F(q,t)$ shows for $q \sim q_p$ the slowest decay (i.e., the broadest half-width) and has for large q-values a rather sharp, needle-like shape. (ii) If we consider an intermediate-temperature state (1373 K)—and this also holds for higher temperature—we again observe oscillations for small q-values which have, however, a much shorter wavelength; these oscillations are extinguished rapidly with increasing q and as low as from $q \sim 0.4$ Å^{-1} onwards $F(q,t)$ is monotonically decreasing. The function then becomes very soon needle shaped with a much smaller half-width than the one observed at 350 K (note also the different time scales in figures 4(a) and 4(b)); furthermore only a much weaker broadening near q_p is observed. At 1873 K the half-width of $F(q,t)$ has become very small and remains nearly unchanged for intermediate and large q-values, no distinct broadening near q_p may be observed.

The above-mentioned behaviour of the half-width of $F(q,t)$ near q_p with increasing temperature may be understood nicely in terms of a very simple *ansatz*. This model, originally devised for hard spheres [52, 53, 54] and generalized to continuous potentials [51, 55] starts from the MF-1 *ansatz* for the Laplace transform $\hat{F}(q,z)$ of the intermediate scattering function $F(q,t)$. Following the arguments of Balucani and co-workers [51, 55], for $q \sim q_p$ $\hat{F}(q,z)$ may be reasonably well approximated by

$$\frac{\hat{F}(q,z)}{S(q)} = \left[z + \frac{\omega_0^2(q)/S(q)}{\omega_l^2(q) - \omega_0^2(q)/S(q)} \frac{1}{\tau_l(q)} \right] \tag{1}$$

and hence

$$F(q,t) = S(q)\mathrm{e}^{-\delta_0(q)t} \qquad \delta_0(q) = \frac{\omega_0^2(q)}{S(q)} \frac{1}{[\omega_l^2(q) - \omega_0^2(q)/S(q)]} \frac{1}{\tau_l(q)}. \tag{2}$$

$\tau_l(q)$ represents a relaxation time, i.e., a parameter which usually is obtained in a least-squares fit to the computer data. Note that if we restrict ourselves furthermore to the simple Lovesey model for $\tau_l(q)$ [26, 56]

$$\frac{1}{\tau_l^L(q)} = \frac{2}{\sqrt{\pi}} \left(\omega_l^2(q) - \frac{\omega_0^2(q)}{S(q)} \right)^{1/2}. \tag{3}$$

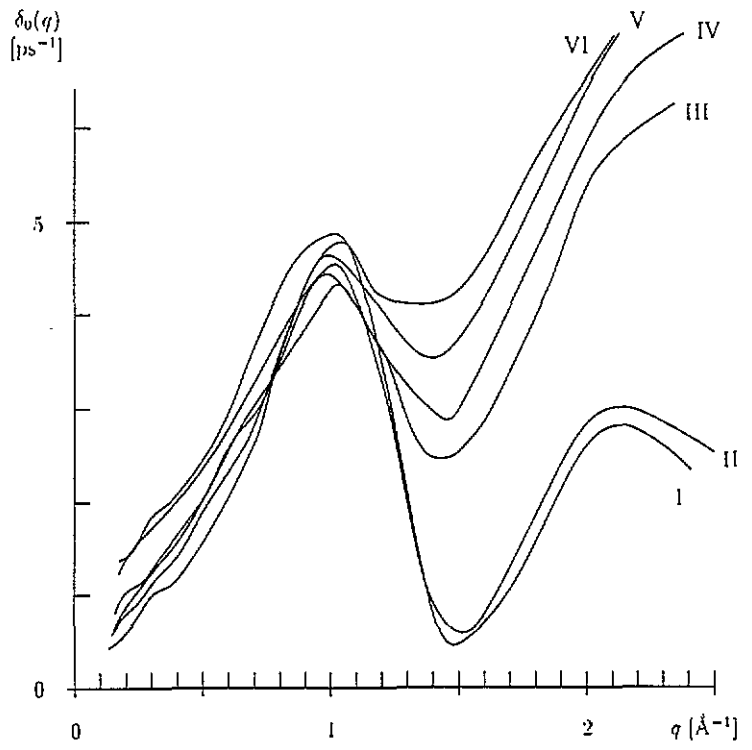

Figure 5. Function $\delta_0(q)$ as defined in equation (2) as a function of q for Rb states I–VI.

$\delta_0(q)$ is entirely determined by static properties of the liquid. The differences between the fitted and the Lovesey values for $\tau_1(q)$ are of rather quantitative than qualitative nature (cf. figure 8(b) and discussion below). In this study, however, we have calculated $\delta_0(q)$ using $\tau_1(q)$ as from an MF-1 fit to the data of $F(q, t)$. $\delta_0(q)$ is depicted in figure 5 and shows as a function of q a similar behaviour as the moments: a pronounced minimum observed for low temperatures near q_p is smeared out as the temperature increases, so that finally for 1873 K only a small dip remains. The position of this minimum (or dip) remains again insensitive to the temperature. According to the simple functional form (2) the curves of δ_0 in figure 5 explain very nicely the two main effects described above. (i) The decreasing half-width near q_p with increasing temperature is explained by the fact that for this q-value the pronounced minimum in $\delta_0(q)$ observed for state I becomes very shallow for state VI. The rather large differences in $\delta_0(q_p)$ between states I and VI mean that density fluctuations decay much faster near q_p for higher temperatures. (ii) The weak (strong) variation of the half-width in $F(q, t)$ for high (or low) temperatures may also be explained by the shallow (deep) minimum of $\delta_0(q)$ near q_p.

In figure 6 we present results for the dynamic structure factor $S(q, \omega)$ for two selected temperatures (1373 and 1873 K). For 350 K (not displayed) a well defined inelastic peak up to $q \sim 1.1$ Å^{-1} is observed while beyond q_p no distinct inelastic peak may be found. The quasielastic peak is sharp and becomes very large in the vicinity of q_p. For intermediate temperatures the side-peak has vanished even for small q-values or is—perhaps—covered by a rather broad central peak ($\omega = 0$); however, we cannot exclude that an inelastic peak may be observed for q-values smaller than those q-values accessible in the computer experiment (cf. figure 1). The half-width of the quasielastic peak is now much broader than for the lower

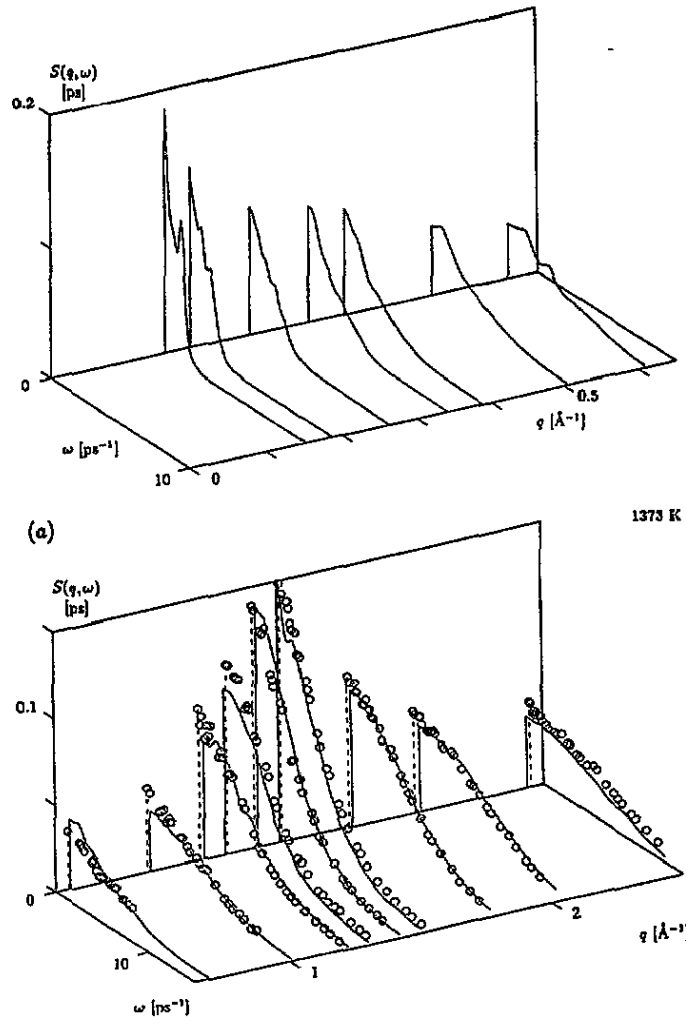

Figure 6. Dynamic structure factors $S(q, \omega)$ as functions of q and ω for the following Rb states: (a) IV (1373 K) and (b) VI (1873 K). Symbols: experimental neutron-scattering results of Winter *et al* [8, 9], full line: computer experiment. The full (broken) vertical lines indicate the theoretical (experimental) q-values.

temperature and near q_p $S(q, \omega)$ decreases much more slowly as a function of ω than at 350 K (cf. also discussion on the half-width of $F(q, t)$ near q_p). For the highest-temperature state at 1873 K, the central peak is for small q-values very sharp and high; it then broadens and its height decreases rapidly as we approach q_p. No inelastic peak can be resolved from the $S(q, \omega)$ data at this temperature. In the comparison between experimental and theoretical results, agreement is found to be excellent up to 1373 K. At 1673 K differences between the two sets of data are small, while they become substantial for the high-temperature state VI. This is obviously—similarly to the differences in the static structure—related to the breakdown of the model for the interatomic forces: in the temperature range where the discrepancies are observed, Rb undergoes a metal/non-metal transition. The change in the electronic structure leads to a change in the interatomic interactions. The state dependence of

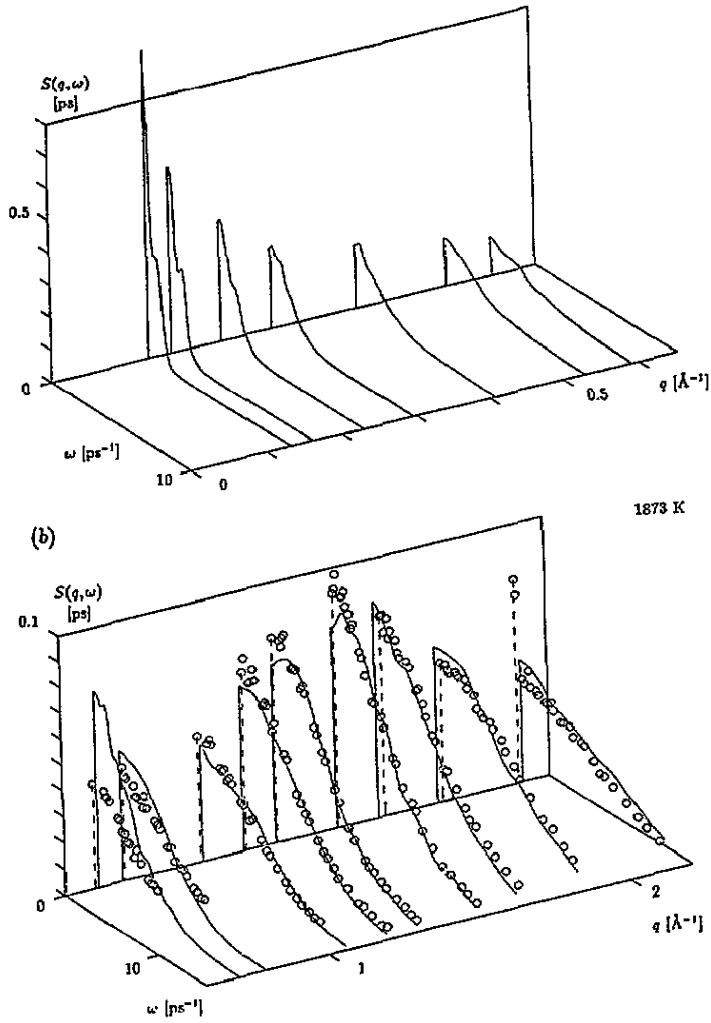

Figure 6. (Continued)

the interatomic forces is also reflected in the asymmetry of the liquid–gas coexistence curve and the violation of the law of the rectilinear diameter over a comparatively large region of densities close to the critical point [57]. It has been shown that the critical behaviour of expanded liquid metals is influenced by this state dependence of the interactions [58]. Interatomic forces constructed from pseudopotentials and linear-response theory depend on the mean electron density, but do not account for the local variations of the forces arising from critical density fluctuations or an inhomogeneous structure of the liquid.

In figure 7 we display the dispersion relation $\omega_l^m(q)$ of the longitudinal current CF $C_l(q,\omega)$ for all six Rb states; a dispersion relation $\omega_B(q)$ for $S(q,\omega)$ could only be determined for the lowest temperatures (states I and II). In the same figure we have also depicted the experimental results of Winter *et al* [8, 9] and the data of Copley and Rowe [6, 7] at a slightly different temperature (320 K). Both the quantitative and the qualitative agreement are found to be very satisfactory. A similar behaviour as observed for the moments (figure 3) and the function $\delta_0(q)$ (figure 5) is encountered for the dispersion

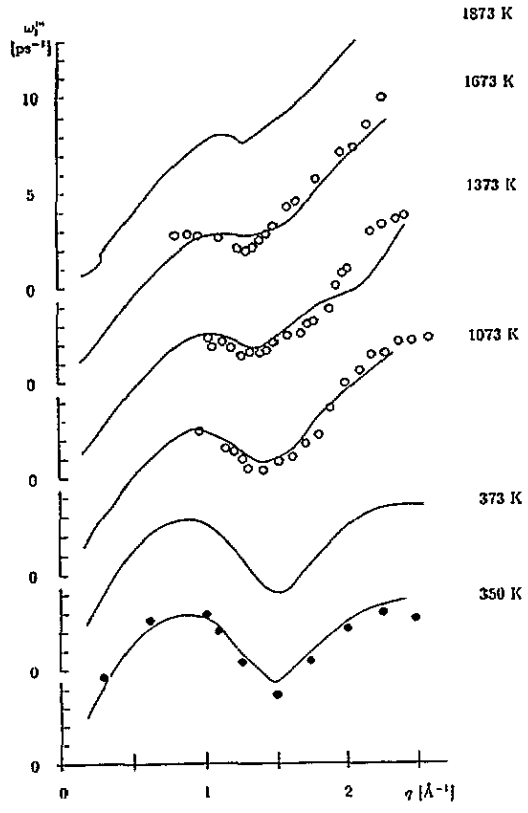

Figure 7. Dispersion relations $\omega_l^m(q)$ of the longitudinal current CFS $C_l(q,\omega)$ as functions of q for Rb states I–VI. Symbols: •, experimental data of Copley and Rowe [6, 7] at a slightly different temperature (320 K); ○, experimental data of Winter *et al* [8, 9]; full line, theoretical results.

$\omega_l^m(q)$ near q_p. We would like to add that model calculations with similar results have also been performed for these quantities [59].

Table 3. Adiabatic velocity of sound c_s as obtained (a) via MC theory (cf. subsection 3.2) and (b) via an HF model for $F(q,t)$ from the computer experiment for Rb states I–VI and the respective experimental values (calculated from thermodynamic properties compiled for Rb on p 508 in [43]).

	c_s (m s^{-1})		
System	Theory (a)	Theory (b)	Experiment
I	1330 ± 60	1100 ± 40	1241
II	1020 ± 60	880 ± 40	1235
III	840 ± 30	830 ± 50	969
IV	850 ± 40	830 ± 40	842
V	780 ± 50	740 ± 50	—
VI	680 ± 50	490 ± 50	—

A simple relation predicted by MC theory which is valid in the low-q region where $\omega_l^m(q)$ and $\omega_B(q)$ differ only marginally [60, 61] ($\omega_l^m(q) \sim \omega_B(q) \sim c_s q + \alpha_s q^{5/2} + O(q^{11/4})$) helps

us to recover a theoretical value for the adiabatic velocity of sound c_s. The coefficient α_s is a measure for the so-called anomal (positive) dispersion relation, encountered both in theory [19, 20] and experiment [10, 11] for temperatures near the melting point for Cs. For states I and II, α_s was indeed found to be positive, for 1073 K the error bar of the α_s-values has already become so large that we are no longer able to claim it to be positive. Finally, for states IV–VI the positivity has disappeared completely and a linear behaviour for small q-values is clearly visible from figure 7. The values obtained for c_s from the above equation, along with another theoretical result and the experimental data (which are available only for states I to IV [43]) are compiled in table 3. Agreement is reasonable and of about the same quality as found for Cs [20].

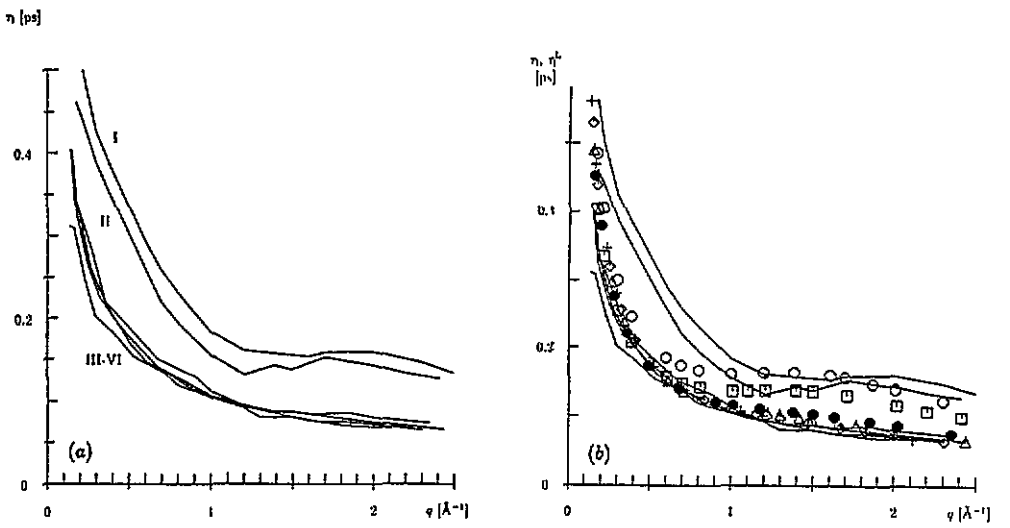

Figure 8. (a) Relaxation time $\tau_1(q)$ of an MF-1 fit to the intermediate scattering function $F(q,t)$ as a function of q for Rb states I–VI. (b) Relaxation time $\tau_1^L(q)$ of an MF-1 model for the intermediate scattering function $F(q,t)$ calculated in the Lovesey model [26, 56] as a function of q; symbols: I, □, II, ○; III, ●; IV, △; V, ◇; VI, +.

We have interpreted the raw computer data of $F(q,t)$ in terms of an HF and two MF models (using one and three model parameters). The generalized, q-dependent parameters appearing in these models have already been listed in subsection 2.3. As a representative of these quantities we have depicted the relaxation time $\tau_1(q)$ of the MF-1 model (figure 8). From this figure—and similar results were encountered for other parameters, too—we observe an interesting tendency: the results for the parameters for the states of intermediate and high temperatures (III–VI) nearly coincide, while the curves of the low-temperature states (I and II) are clearly separated from these data. Since on the other hand drastic changes in the dynamic CFs have been observed as we increase the temperature we have to make a more detailed investigation of via which channels temperature may enter these dynamic CFs. To this end we make again recourse to the above-mentioned simple MF-1 model which in general describes the dynamic CFs quite accurately; this model is built up by: (i) the q-dependent moments; they are calculated from the static properties and here temperature enters via the PDF and the interatomic potentials; (ii) the q-dependent parameters of the model; they are obtained in a least-squares fit to the dynamic CFs of the computer experiment.

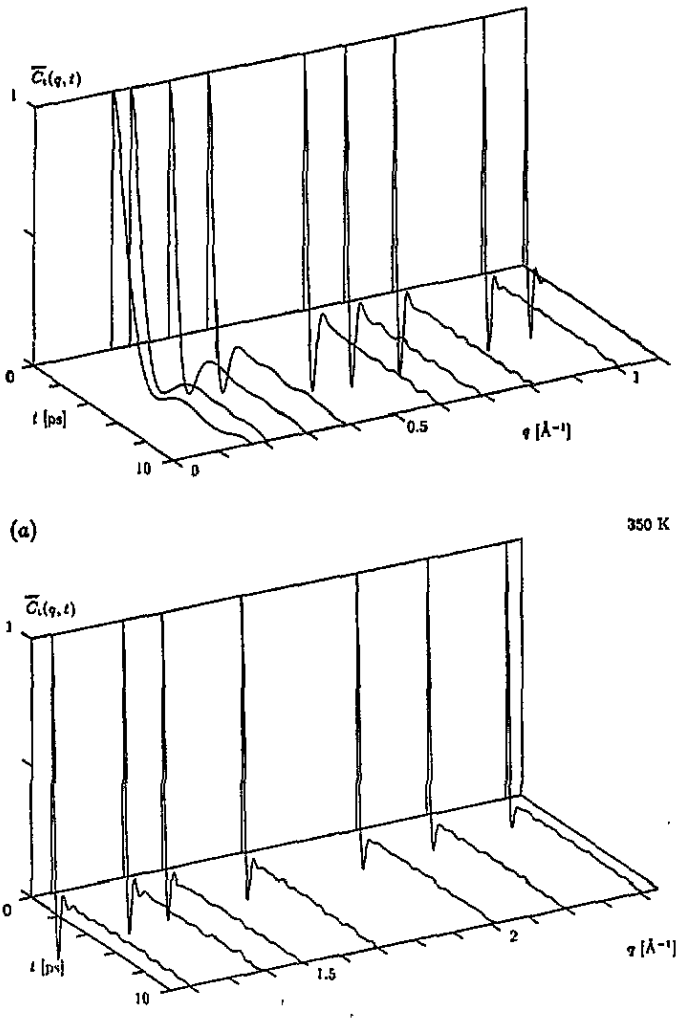

Figure 9. Normalized transverse current CFs $\bar{C}_t(q,t) = C_t(q,t)/\tilde{\omega}_t^0(q)$ as functions of q and t for the following Rb states: (a) I (350 K) and (b) IV (1373 K).

Obviously, for states I and II temperature enters via both channels. For the states III–VI, however, the temperature dependence of the dynamic CFs is *entirely* determined by the moments since—within numerical accuracy—no temperature dependence of τ_l could be observed for these four states. Interestingly enough, our results for the numerically determined parameter τ_l are assessed by the Lovesey model ($\tau_l^L(q)$) (cf. (3)) [26, 56], both in a qualitative and quantitative way. We have depicted $\tau_l^L(q)$ in figure 8(b) for states I–VI along with the numerically determined fitting parameter $\tau_l(q)$: for states III–VI the data practically coincide, while differences for states I and II are visible which marks the limits of the Lovesey model. Let us consider once more the prescription of how to determine $\tau_l^L(q)$ (equation (3)): it is worthwhile mentioning that—although all the functions required in this expression are highly temperature *dependent*—the results for states III–VI are practically temperature *independent*.

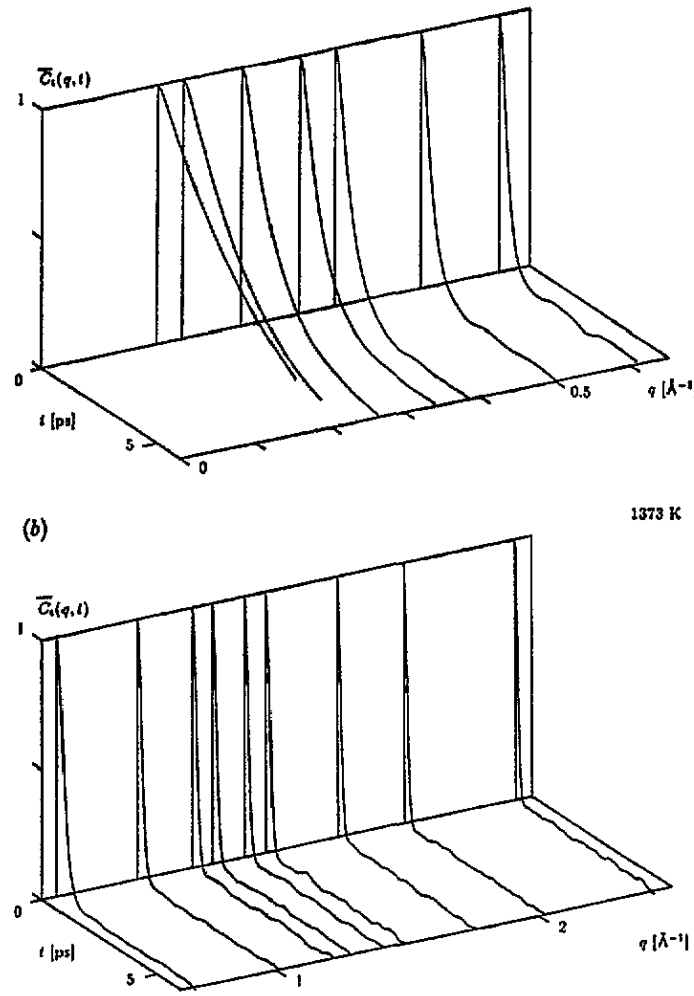

Figure 9. (Continued)

3.2.2. Transverse current correlation functions. The transverse current CFs $C_t(q,t)$ are accessible only in the computer experiment. In figure 9 we have depicted results for $C_t(q,t)$ for two selected states (350 K and 1373 K). Again, similarly to $F(q,t)$ drastic differences between low- and high-temperature states may be observed: the pronounced oscillations, encountered over the entire q-range for 350 K, are completely extinguished for the high-temperature state: $C_t(q,t)$ becomes a simple monotonically decreasing function in time t; the half-width of $C_t(q,t)$ is for all states—in contrast to $F(q,t)$—monotonically decreasing as a function of q. Only for the low temperatures may a slight broadening be observed. For intermediate and high temperatures the transverse dynamic behaviour becomes rather insensitive to temperature.

The transverse dispersion relation $\omega_t^m(q)$ for states I–VI is depicted in figure 10; despite the kinks in the curves which reflect the difficulties in properly determining the side peak, results are accurate enough to observe that the q-vector from which point transverse collective modes may be observed (q_t) increases nearly in a linear way with temperature.

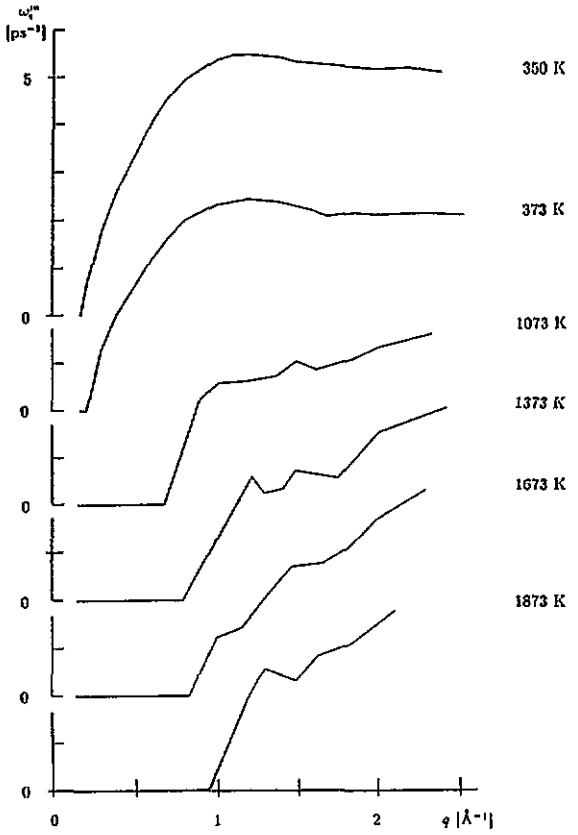

Figure 10. Dispersion relations $\omega_t^m(q)$ of the transverse current CFS $C_t(q, \omega)$ as functions of q for Rb states I–VI.

The transverse velocity of sound c_t, defined for q near q_t via $c_t^m \sim (q - q_t)\omega_t^m(q)$ and q_t are compiled in table 4. In the 1980s, MD simulations for the determination of dynamic properties of both LJ systems and liquid metals have revealed the following: in liquid metals (both slightly below the respective melting points: Na—293 K and K—300 K) the regions up to where longitudinal collective modes (q_l) and from where on transverse collective modes (q_t) may be observed do overlap; for LJ systems, however, it was observed that $q_l < q_t$, i.e., there exists a q-gap where neither longitudinal nor transverse modes can propagate. Estimates of q_l and q_t in terms of r_p (defined above) have been given by Jacucci and McDonald [62] but could not be verified to hold over the entire temperature range. Furthermore, we encounter for *expanded* liquid metals a situation similar to LJ systems: we observe the existence of a region where neither longitudinal nor transverse collective modes may propagate: in our experiment we find that q_l becomes smaller than q_t; in fact for the intermediate and high temperatures q_l is well below the smallest q-value available in the simulation. Finally we want to point out that our q_t-curves merge nicely into the data obtained by Mountain [16] for temperatures near the melting point.

Again, the computer data for $C_t(q, t)$ have been studied in terms of an HF and of two MF models. If we look at $C_t(q, t)$ depicted in figure 9 and take into account the functional form of the HF model, i.e., $C_t(q, t) = \omega_t^0(q)e^{-\nu q^2 t}$ it is obvious that the quality of this HF fit to an oscillating $C_t(q, t)$ cannot be satisfactory for states I and II: in fact, least-squares

Table 4. q_t, the q-vector from whereon transverse collective modes are supported, and c_t, the transverse velocity of sound, (both as defined in the text) for Rb states I–VI.

System	q_t (Å^{-1})	c_t (m s^{-1})
I	0.170	1382
II	0.203	1137
III	0.665	810
IV	0.716	501
V	0.833	757
VI	0.926	708

sums (LSQs) of up to five are observed. Only for states III–VI where all the oscillations in time have vanished do we get LSQs of below one.

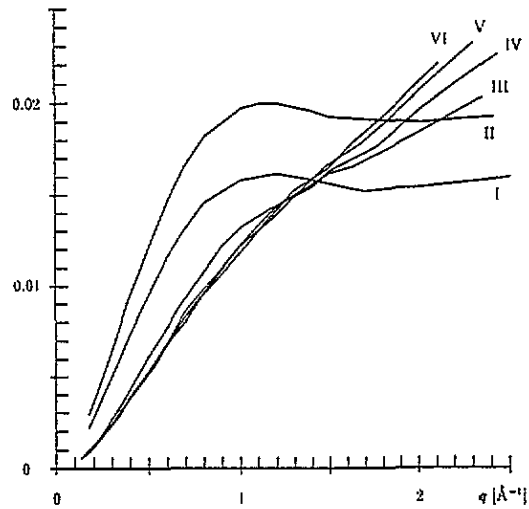

Figure 11. Dimensionless generalized kinetic shear viscosity $\nu^*(q) = \nu(q)q^2\Delta t$ ($\Delta t = 3$ fs) as a function of q obtained in an HF fit to the transverse current CF $C_t(q, t)$ for Rb states I to VI.

In figure 11 we have displayed the reduced dimensionless kinetic shear viscosity $\nu^* = \nu q^2 \Delta t$ ($\Delta t = 3$ fs) as a function of q for states I–VI. Similarly as observed for the model parameters for $F(q, t)$ we find clearly separated curves for the low temperatures, while again the results of states III–VI practically coincide. This also holds for $\tau_t(q)$, the relaxation time of the MF-1 model, displayed in figure 12. Again this means that temperature effects in the transverse dynamic structure may enter only via the static moment $\omega_t^2(q)$. However, since this moment is much less temperature dependent than the longitudinal moment $\omega_l^2(q)$ (cf. figure 3) this also explains the small quantitative differences in $C_t(q, t)$ observed for intermediate and higher temperatures and discussed above (cf. figure 9).

If we compare the results for the parameters of the MF-1 and MF-3 models, we observe for *all* temperatures the following: for small q-values two different relaxation times $\tau_{t1}(q)$ and $\tau_{t2}(q)$ were obtained in the MF-3 model; they differ approximately by one order of magnitude. Near $q \sim 0.4$ Å^{-1}—and this is rather insensitive of temperature—the smaller

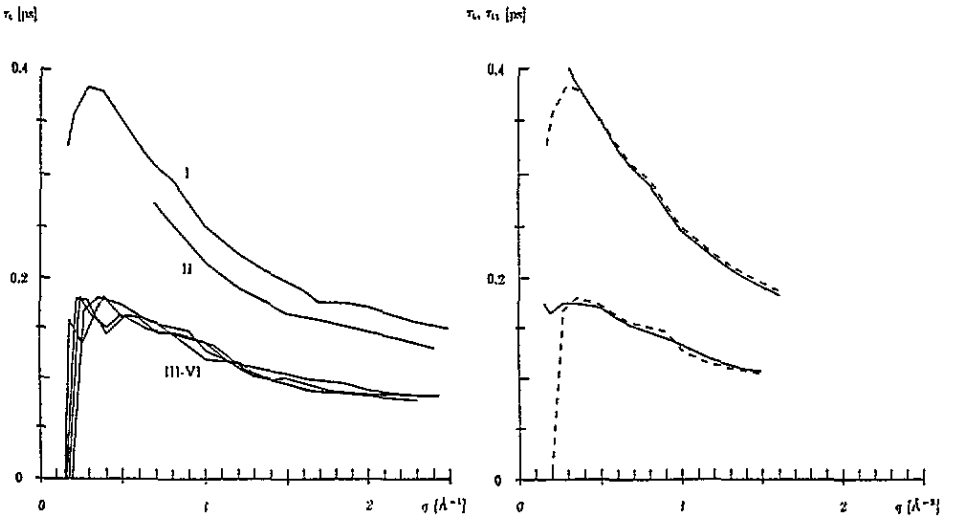

Figure 12. Relaxation times $\tau_t(q)$, and $\tau_{t1}(q)$ (broken line in the right panel) as functions of q as obtained in an MF-1 or MF-3 fit, respectively to the transverse current CF $C_t(q, t)$ for Rb states I–VI; the right panel displays the curves for states I (top) and III (bottom).

relaxation time (say $\tau_{t1}(q)$) merges into the curve of $\tau_t(q)$, i.e., the relaxation time of the one-parameter model. Hence, we conclude that for low q-values we have two mechanisms to describe the decay of transverse modes: a fast ('binary') and a slow ('collective') one. As we increase q, the slow relaxation process vanishes completely, i.e., the decay of the transverse modes is entirely supported by the fast 'binary' process. Similar observations have also been made by the present authors for liquid Cs near the melting point [20, 63] and by Balucani *et al* for low temperatures [17, 18].

Table 5. (a) Diffusion constant D in 10^{-8} m^2 s^{-1} as obtained from the mean square displacement ($D = \lim_{t\to\infty}(1/6t)\langle|r(t) - r(0)|^2\rangle$) from the computer experiment for Rb states I–VI and the respective experimental values (p 845 in [43]; cf. discussion in the text). (b) Specific heat at constant volume C_v as obtained from the temperature fluctuations in the computer experiment (cf. (51) of [20]) for Rb states I–VI and the respective experimental values (taken from a table on p 508 in [43]).

	D (m^2 s^{-1}) $\times$ 10^{-8}		C_v (J g^{-1} K^{-1})	
System	*Theory*	*Experiment*	*Theory*	*Experiment*
I	$0.305 \pm (0.4 \times 10^{-4})$	0.352 ± 0.01	0.318 ± 0.03	0.336
II	$0.378 \pm (0.6 \times 10^{-4})$	0.418 ± 0.02	0.326 ± 0.02	0.332
III	$3.59 \pm (0.6 \times 10^{-3})$	3.66 ± 1.8	0.215 ± 0.01	0.251
IV	$5.86 \pm (0.9 \times 10^{-3})$	6.05 ± 4.4	0.199 ± 0.01	0.229
V	$8.56 \pm (0.8 \times 10^{-3})$	9.35 ± 8.4	0.187 ± 0.01	—
VI	$12.5 \pm (0.2 \times 10^{-2})$	14.2 ± 15	0.184 ± 0.01	—

3.3. Thermodynamic and elastic properties

Again—as already observed in our previous study on liquid Cs [20]—it has turned out that a proper and *reliable* determination of several elastic and thermodynamic properties

from the computer experiment is extremely difficult. The most reliable results may in general be obtained for those quantities which can be determined directly from the computer experiment, such as the diffusion constant (from the mean square displacement) and the specific heat (from the temperature fluctuations), both compiled in table 5. The main problem in a proper determination of these quantities is caused by the difficulties in finding the best but at the same time a reliable fit to the computer data (cf. discussion in [20]). In this contribution extrapolations towards $q = 0$ have been performed using linear/quadratic/cubic least-squares fits, including four/six/eight q-points; if the sum of the least squares is of a reasonable size then – according to our experience—in general, the resulting three data are rather consistent. The errors noted in the tables express these deviations from the mean value.

(i) The adiabatic velocity of sound c_s has already been discussed above (cf. subsection 3.2 and table 3).

(ii) The specific heat C_v was obtained from the temperature fluctuation recorded during the simulation via equation (51) of [20]. In the tables of [43], experimental values for C_v are tabulated only for a temperature range covering states I to IV. The differences between theory and experiment are on the average 10–15%.

(iii) The diffusion constant D has been determined from the mean square displacement recorded during the simulation. The discussion of the results turns out to be rather delicate: Tanaka [48] observed in his study on the *static* properties of expanded Rb (where he also calculated the diffusion constant), that 'the computed value of D is rather sensitive to the choice of the pair potential'. In fact, in a direct comparison between these two theoretical studies we find for two comparable states (i.e., states III and VI of *this* study) differences of 10 and 15%. In table 5 we have tried to present a comparison between theoretical and experimental results for D. Concerning the experimental data for the diffusion constant the following has to be mentioned: in [43] (p 845) three interpolation formulae for D as functions of T are proposed which are supposed to give a recipe for the determination of an experimental value for D. However, no limitations are marked concerning their validity in temperature. The value listed in the 'experiment' column of table 5 is the average over these three expressions, the error is determined from the deviation from this mean value. The large errors of the last two or three states indicate that we have obviously exceeded the range of validity of at least one of these three expressions.

In an effort to assess our results we have then looked for other possibilities for determining D. Balucani *et al* [21, 22] determined their transport coefficients via a generalized Green–Kubo formalism and arrive at a universal expression for all alkali metals $D = (\sigma^2/\tau)T^*D^*$ where T^* is the reduced temperature, σ and τ are length and time units characteristic for the state and the metal. D^* is some 'universal' simulation constant. Although this equation seems to give good results for all alkali metals near the melting point, it could not reproduce our results over this large temperature range.

We have tried an analysis of D in terms of the half-width $\omega_0^{1/2}(q)$ of the quasielastic peak of $S(q, \omega)$, as proposed in [50]. It is suggested that near q_p, $\omega_0^{1/2}(q)$ can be described in a reliable way by $\omega_0^{1/2}(q) = D_E q^2 d(q)[S(q)]^{-1}$ and $d(q) = [q - j_0(x) + 2j_2(x)]^{-1}$, the $j_i(x)$ being the spherical Bessel functions of order i and $x = q\sigma$; D_E is the Enskog diffusion constant. σ is a hard-core diameter not specified more closely. Winter *et al* [8, 9, 34] used this expression to determine D_E from their results. A similar interpretation of our data showed that the ambiguity in the definition of σ yields a rather large uncertainty in the actual value of D_E: variation in σ by 10% around the first node in $\Phi(r)$ causes differences in D_E of 20%. If we take σ to be the first zero in $\Phi(r)$, we obtain reasonable agreement with our theoretical results for D of states III–V listed in table 5.

(iv) The sound attenuation coefficient Γ and the thermal diffusivity D_T have both been determined from the HF parameters to $F(q,t)$. Experimentally D_T is determined from the heat conductivity κ via $D_T = \kappa/(\rho C_p)$, C_p being the specific heat at constant pressure; Γ may then be obtained via $\Gamma = \frac{1}{2}(D_T(\gamma - 1) + \eta_l/\rho M)$, with $\gamma = C_p/C_v$ and η_l being the longitudinal viscosity. However, in metals the largest contribution to the heat conductivity stems from the electrons, while phonons contribute only to a minor extent. Bodensteiner [10] has estimated that for liquid Cs just above the melting point the contribution of the phonons to the heat conductivity (which we obtain from the computer experiment) is of about two orders of magnitude smaller than the macroscopic value. Similar results have been summarized by Shimoji [64].

(v) Finally the kinetic shear viscosity ν may be determined both from an HF-fit and an MF-1-fit to $C_t(q,t)$. For the determination of ν we found the best internal consistency for the computer experiment as well as the best agreement with experiment among all thermodynamic and elastic properties discussed in this section. Theoretical values obtained via both routes are compiled along with the experimental values in table 6. Only for the low-temperature states are differences from the experiment observed: this becomes clear if we consider what we have noted above on the inadequacy of a simple non-oscillating HF model to describe $C_t(q,t)$ which shows oscillations in time for low temperatures. However, as we increase the temperature $C_t(q,t)$ becomes a simple monotonically decaying function, and may therefore be approximated very well by the Gaussian shape of the HF model. The observed LSQ values are of reasonable size and hence the values for ν have to be considered as reliable.

Table 6. Kinetic shear viscosity ν in 10^{-6} m^2 s^{-1} as obtained from the computer experiment ((a): HF fit and (b) MF-1 fit to $C_t(q,t)$) for Rb states I–VI and the respective experimental values (taken from a table on p 781 in [43]).

	ν (m^2 s^{-1}) $\times 10^{-6}$		
System	Theory (a)	Theory (b)	Experiment
I	0.430 ± 0.02	0.416 ± 0.01	0.326
II	0.384 ± 0.02	0.367 ± 0.01	0.301
III	0.103 ± 0.005	0.095 ± 0.005	0.120
IV	0.117 ± 0.005	0.117 ± 0.005	0.114
V	0.124 ± 0.005	0.123 ± 0.005	0.120
VI	0.124 ± 0.005	0.121 ± 0.005	0.136

Concluding this subsection, we would like to point out that the good results obtained for ν are—unfortunately—not the rule; in the determination of thermodynamic and elastic quantities we rather have to expect typically uncertainties and error bars such as those encountered for the other quantities.

4. Conclusion

In this contribution we have reported on a computer experiment for the determination of the dynamic properties of liquid rubidium, investigated over a temperature range from above the melting point up to near the critical temperature (1873 K). The present paper—the first of two contributions—is concerned with collective CFs and related quantities only. Four of the

investigated states are exactly those as considered recently in a neutron-scattering experiment by Winter and co-workers. For both the static and dynamic structure we find good qualitative and quantitative agreement between theory and experiment up to intermediate temperatures. Only for the highest-temperature state are substantial discrepancies observed. They may be attributed to the simple model for the interatomic forces, i.e., a potential based on an Ashcroft empty-core pseudopotential: this model depends only on the mean electronic density and hence is not able to take into account local variations of the forces arising from critical density fluctuations or an inhomogeneous structure of the liquid, both encountered in the vicinity of the critical point, where Rb undergoes a metal/non-metal transition. Both, $F(q,t)$ and $S(q,\omega)$ show in the vicinity of q_p a characteristic broadening: in both cases the half-widths turn out to be strongly temperature dependent. This effect—known as the de Gennes narrowing—may be understood both qualitatively and quantitatively in terms of rather simple models based entirely on *static* properties. This narrowing is also reflected in the behaviour of some characteristic functions in q near q_p (dispersion relations, static moments): they show for low temperatures pronounced minima or maxima, which become smeared out for higher temperatures. Good agreement between theory and experiment is also observed for the longitudinal dispersion relation $\omega_l^m(q)$, determined from the longitudinal current CFs (an inelastic peak of $S(q,\omega)$ may be recovered only for low temperatures). Only for the lowest temperatures (states I and II) the dispersion turns out to be *anomalous* (positive enhancement over the linear behaviour described by the velocity of sound); for the other states, a clear *linear* dispersion may be observed. The model parameters of the HF and the MF models become temperature independent for intermediate and high temperatures and practically coincide, while the lower-temperature curves are clearly separated. This means, that—in terms of these models—the temperature influence on these CFs may enter only via the static moments.

Similar—though much weaker—characteristic differences between low- and high-temperature states are observed for the transverse current CFs $C_t(q,t)$. Transverse collective modes may only be supported from (a non-zero) q_t onwards. For low temperatures we find an overlap of the regions up to where longitudinal collective modes are observed ($q < q_l$) and from where on transverse collective modes are encountered ($q > q_t$); for higher temperatures, however, a gap between q_l and q_t (i.e., $q_l < q_t$) is found, similar to the gap observed for Lennard-Jones systems. From the results of one- and three-parameter MF-model calculations for $C_t(q,t)$ we can conclude that for low q-values (i.e., typically less than 0.4 Å^{-1}), two mechanisms can be made responsible for the decay of transverse modes: a fast 'binary' and a slow 'collective' one; for higher q-values only the fast process survives, the slow one being completely extinguished: these results are observed for all temperatures investigated.

Once more it has been confirmed that a *reliable* and *accurate* determination of several elastic and thermodynamic properties from the computer experiment is extremely difficult and sometimes turns out to be even impossible. Differences between theoretical and experimental data (which, in turn, are rather difficult to obtain in particular for the higher temperatures) are in general of about 15–20%. Several quantities, such as the sound attenuation coefficient or the thermal diffusivity have—apart from the phonon contribution—an important electronic contribution. In these cases a direct comparison with the computer-simulation results (which gives us the phonon contribution only) is not possible. In general we think that a determination of the thermodynamic and elastic properties in terms of a generalized Green–Kubo formalism seems to be a more reliable approach.

Acknowledgments

The authors would like to thank Professor J Hafner (Wien) for many interesting and stimulating discussions and useful hints. Special thanks are due to Professor R Winter (Dortmund) for providing detailed experimental data [7, 8] (partly prior to publication) and for useful discussions. This work was supported by the Österreichische Forschungsfonds under project No P8912-PHY and the Oesterreichische Nationalbank under project No 4649.

References

[1] de Jong P H K, Verkerk P, Ahda S and de Graaf L A 1992 *Recent Developments in the Physics of Fluids* ed W S Howells and A K Soper (Bristol: Hilger) p F233
[2] de Jong P H K, Verkerk P and de Graaf L A 1993 *J. Non-Cryst. Solids* **156–158** 48
[3] Montfroy W, de Schepper I M, Bosse J, Glaser W and Morkel C 1986 *Phys. Rev.* A **33** 1405
[4] Morkel C and Gläser W 1986 *Phys. Rev.* A **33** 3383
[5] Morkel C, Gronemeyer C, Gläser W and Bosse J 1987 *Phys. Rev. Lett.* **58** 1873
[6] Copley J R D and Rowe J M 1974 *Phys. Rev. Lett.* **32** 49
[7] Copley J R D and Rowe J M 1974 *Phys. Rev.* A **9** 1656
[8] Pilgrim C, Winter R, Hensel F, Morkel C and Gläser W 1992 *Recent Developments in the Physics of Fluids* ed W S Howells and A K Soper (Bristol: Hilger) p F181
[9] Winter R, Pilgrim C, Hensel F, Morkel C and Gläser W 1993 *J. Non-Cryst. Solids* **156–158** 9
[10] Bodensteiner T 1990 *PhD Thesis* Technische Universität München
[11] Morkel C and Bodensteiner T 1990 *J. Phys.: Condens. Matter* **2** SA251
[12] Bodensteiner T, Morkel C, Gläser W and Dorner B 1992 *Phys. Rev.* A **25** 5709
[13] Rahman A 1974 *Phys. Rev.* A **4** 1667
[14] Rahman A 1974 *Phys. Rev. Lett.* **32** 52
[15] Haan S W, Mountain R D, Hsu C S and Rahman A 1980 *Phys. Rev.* A **22** 767
[16] Mountain R D 1982 *Phys. Rev.* A **26** 2859
[17] Balucani U, Vallauri R and Gaskell T 1987 *Phys. Rev.* A **35** 4263
[18] Balucani U and Vallauri R 1989 *Phys. Rev.* A **40** 2796
[19] Kambayashi S and Kahl G 1992 *Europhys. Lett.* **18** 421
[20] Kambayashi S and Kahl G 1992 *Phys. Rev.* A **46** 3255
[21] Balucani U, Torcini A and Vallauri R 1993 *Phys. Rev.* B **47** 3011
[22] Balucani U, Torcini A and Vallauri R 1992 *Phys. Rev.* A **46** 2159
[23] Canales M, Padró J A, Gonzalez L E and Giró A 1993 *J. Phys.: Condens. Matter* **5** 3095
[24] Nowotny G, Kahl G, and Hafner J 1994 *Phys. Scr.* at press
[25] Boon J-P and Yip S 1980 *Molecular Hydrodynamics* (New York: McGraw-Hill); 1991 *Molecular Hydrodynamics* (New York: Dover)
[26] Hansen J-P and McDonald I R 1986 *Theory of Simple Liquids* 2nd edn (London: Academic)
[27] Hensel F 1990 *J. Phys.: Condens. Matter* **2** SA33
[28] Hensel F 1990 *J. Non-Cryst. Solids* **117 & 118** 441
[29] Hensel F and Uchtmann H 1989 *Annual Rev. Phys. Chem.* **40** 61
[30] Freyland W 1979 *Phys. Rev.* B **20** 5104
[31] El Hanany W, Brennert G F and Warren W W 1983 *Phys. Rev. Lett.* **50** 540
[32] Knuth B and Hensel F 1990 *High Pressure Res.* **5** 552
[33] Franz G, Freyland W, Gläser, Hensel F and Schneider E 1980 *J. Physique Coll.* **41** C8 194
[34] Winter R, Bodensteiner T, Gläser W and Hensel F 1987 *Ber. Bunsenges. Phys. Chem.* **91** 1327
[35] Winter R and Hensel F 1989 *Phys. Chem. Liq.* **20** 1
[36] Redmer R, Reinholz H, Röpke G, Winter R, Noll F and Hensel F 1992 *J. Phys.: Condens. Matter* **4** 1659
[37] Hoshino K, Matsuda N, Mori H and Watabe M 1990 *J. Non-Cryst. Solids* **117 & 118** 44
[38] Kahl G and Hafner J 1984 *Phys. Rev.* A **29** 3110
[39] Kahl G 1994 *J. Phys.: Condens. Matter* **6** 10923
[40] Ashcroft N W 1966 *Phys. Lett.* **23** 48
[41] Ichimaru S 1982 *Rev. Mod. Phys.* **54** 1027
[42] Ichimaru S and Utsumi K 1982 *Phys. Rev.* B **24** 7381

[43] Ohse R (ed) 1985 *Handbook of Thermodynamic and Transport Properties of Alkali Metals* (Oxford: Blackwell)
[44] Hafner J 1987 *From Hamiltonians to Phase Diagrams* (Berlin: Springer)
[45] Copley J R D and Brockhouse B N 1973 *Can. J. Phys.* **51** 657
[46] Moriarty J A 1982 *Phys. Rev.* B **26** 1754
[47] Arnold A, Mauser N and Hafner J 1989 *J. Phys.: Condens. Matter* **1** 965
[48] Tanaka M 1980 *J. Phys. F: Met. Phys.* **10** 2581
[49] de Gennes P-G 1959 *Physica* **25** 825
[50] Cohen E G D, Westerhuijs P and de Schepper I M 1987 *Phys. Rev. Lett.* **59** 2872
[51] Balucani U and Vallauri R 1989 *Phys. Rev.* A **40** 2796
[52] de Schepper I M and Cohen E G 1982 *J. Stat. Phys.* **27** 223
[53] Kirkpatrick T R and Niewoudt J C 1986 *Phys. Rev.* A **33** 2651
[54] Kirkpatrick T R and Niewoudt J C 1986 *Phys. Rev.* A **33** 2658
[55] Balucani U, Vallauri R and Gaskell T 1990 *Nuovo Cimento* D **12** 511
[56] Copley J R D and Lovesey S W 1975 *Rep. Prog. Phys.* **38** 461
[57] Jungst S, Knuth B and Hensel F 1989 *Phys. Rev. Lett* **55** 2160
[58] Goldstein R E and Ashcroft N W 1989 *Phys. Rev. Lett.* **55** 2164
[59] Hoshino K, Ugawa H and Watabe M 1992 *J. Phys. Soc. Japan* **61** 2182
[60] Ernst H and Dorfman J R 1972 *Physica* **61** 157
[61] Ernst H and Dorfman J R 1975 *J. Stat. Phys.* **12** 311
[62] Jacucci G and McDonald I R 1980 *Mol. Phys.* **39** 515
[63] Kahl G, Kambayashi S and Nowotny G 1993 *J. Non-Cryst. Solids* **156–158** 15
[64] Shimoji M 1977 *Liquid Metals* (London: Academic)